


Myxomas and myxoid liposarcomas of the extremities: Our preliminary findings in conventional, perfusion, and diffusion magnetic resonance

Acta Radiologica Open
11(10) 1–11
© The Author(s) 2022
Article reuse guidelines:
sagepub.com/journals-permissions
DOI: 10.1177/20584601221131481
journals.sagepub.com/home/arr


Luz M Morán¹ , Jesús Vega² , Nieves Gómez-León³ and Ana Royuela⁴

Abstract

Background: The differentiation between myxomas and myxoid liposarcomas (MLPS) often is a serious challenge for the radiologists. Magnetic resonance imaging (MRI) is the most useful imaging technique in characterization of the soft tissue tumors (STT).

Purpose: To evaluate in a sample of myxomas and MLPS of the extremities, what morphological findings in conventional MRI allow us to differentiate these two types of myxoid tumors, in addition to analyzing the validity of the apparent diffusion coefficient (ADC) values of diffusion-weighted MRI (DW-MRI).

Material and Methods: Magnetic resonance imaging studies in myxomas and MLPS of extremities searched in our PACS between 2015 and 2019. All studies had conventional MRI with T1, T2, and PD SPAIR sequences, while DW-MRI with ADC mapping and perfusion MRI with a T1 sequence repeated for 4 minutes after contrast injection were additional sequences only in some explorations. Two radiologists evaluated independently the MRI studies by examining the qualitative parameters. Apparent diffusion coefficient values were calculated using two methods—ADC global and ADC solid, and Receiver Operating Characteristic (ROC) curves were applied for analysis.

Results: The features were consistent with MLPS: size greater than 10 cm, heterogeneous signal on T1, and nodular enhancement, while the common findings for myxomas were a homogeneously hypointense signal on T1 and diffuse peritumoral enhancement. The solid and global ADC values were higher in myxomas. We observed that the solid ADC value less than $2.06 \times 10^{-3} \text{ mm}^2 \times \text{s}$ would support the diagnosis of MLPS against myxoma.

Conclusion: Overall, MRI with its different modalities improved the diagnostic accuracy when differentiating myxomas from MLPS of extremities.

Keywords

soft tissue tumors, myxoma, myxoid liposarcoma, magnetic resonance imaging, diffusion-weighted MRI, apparent diffusion coefficient

Received 8 February 2022; accepted 22 September 2022

¹Department of Radiology, Hospital Universitario Puerta de Hierro, Majadahonda, Madrid, Spain

²Department of Pathology, Hospital Universitario Clínico San Carlos, Madrid, Spain

³Department of Radiology, Hospital Universitario La Princesa, Madrid, Spain

⁴Department of Statistics, Hospital Universitario Puerta de Hierro, Majadahonda, Madrid, Spain

Corresponding author:

Luz M Morán, Department of Radiology, Hospital Universitario Puerta de Hierro, C/Manuel de Falla, Majadahonda, Madrid 28300, Spain.

Email: lmoran.moran6@gmail.com



Creative Commons Non Commercial CC BY-NC: This article is distributed under the terms of the Creative Commons Attribution-NonCommercial 4.0 License (<https://creativecommons.org/licenses/by-nc/4.0/>) which permits non-commercial use, reproduction and distribution of the work without further permission provided the original work is attributed as specified on the SAGE and Open Access pages (<https://us.sagepub.com/en-us/nam/open-access-at-sage>).

Introduction

Myxoid tumors are neoplasms of mesenchymal origin characterized by a gelatinous appearance for their matrix rich in glycosaminoglycans, which capture and retain water.¹ Benign and malignant myxoid tumors show considerable clinical and imaging overlap, and their differentiation often poses a serious challenge for the radiologist. This difficulty is particularly common when differentiating myxomas from myxoid liposarcomas (MLPS).

Myxoma is one of the most frequent benign myxoid tumors, with 0.1–0.13 cases per 100,000 inhabitants.² Myxoid liposarcomas is not exceptional, accounting for 15–20% liposarcomas and for 5% of all soft tissue sarcomas in adults.³

The differentiation between these tumors can also pose a serious challenge for the pathologist, who, when doubting morphological findings, relies on molecular biology and on radiological diagnosis. These molecular biology techniques analyze the fused in sarcoma—DNA-damage-inducible transcript 3 (FUS-DDIT3) and t (12, 16) (q13; p11) translocations present in MLPS.

From a histological standpoint, myxoma is a hypovascular lesion with low cellularity, without atypia or mitotic figures, whereas MLPS is characterized by abundant lipoblasts and a prominent vascular network.⁴ Macroscopically, myxomas and MLPS show a fibrous pseudocapsule, but at the microscopic level, the myxoma infiltrates the adjacent muscle tissue.

Magnetic resonance imaging (MRI) is generally the first-line imaging test in the study of soft tissue tumors (STT), followed by ultrasound (US) and computed tomography (CT). Magnetic resonance imaging makes it possible to characterize MLPS when identifying small nodules or septa of fat within the myxoid matrix.⁵ In contrast, diffusion-weighted MRI (DW-MRI) estimates the degree of cellularity of these tumors by analysis of diffusion restriction and apparent diffusion coefficient (ADC) mapping. In general, lower ADC map values indicate malignancy; however, these results remain controversial in STT, most likely due to the heterogeneity of these tumors.^{6–10}

We have collected data on extremities myxomas and MLPS, diagnosed in our hospital, in the last 6 years, and analyzed the MRI studies performed in these patients for the initial diagnosis of these tumors. In DW-MRI studies, we have analyzed their ADC values and compared them with the values reported in the literature; Einarsdottir and colleagues found no significant differences in ADC values between benign and malignant STT, but they observed that MLPS and intramuscular myxoma were the sarcoma and benign tumor with the highest ADC values.⁶ Maeda explained these results based on the free water content of the extracellular matrix of myxoid tumors.⁸ Nagata found significant differences in ADC values between malignant and benign STT, albeit when excluding myxoid tumors

from the study.⁹ In recent works, no significant differences have been found in ADC values between malignant and benign myxoid STT.^{11–15}

We aimed to analyze different MRI parameters in our series when characterizing myxomas and MLPS in extremities. We examined the differential morphological findings and ADC values of DW-MRI in these two myxoid tumors, and comparing two systems for calculating the ADC value and our results with those reported in the literature.

Material and methods

This retrospective observational study was approved by the Research Ethics Committee of the hospital under file PI-222/19.

Study population

Magnetic resonance imaging studies conducted in patients with myxomas and MLPS in extremities, treated between 2015 and 2019, were searched in PACS, using the following inclusion criteria: histological diagnosis of myxoma or myxoid liposarcoma and confirmed by biopsy or surgical specimen. The following exclusion criteria were applied: MRI studies not performed at the time of tumor diagnosis but at post-treatment follow-up.

Clinical data collection

Clinical data were retrieved from the Electronic Health Record Systems without changing data or directly contacting any patient. The following clinical variables were assessed: age, sex, location of the lesion (upper or lower limbs), presence of mass, pain and/or inflammatory signs at the time of diagnosis, and time elapsed from the onset of symptoms to MRI.

MR image acquisition

Magnetic resonance imaging studies were performed on a 1.5 T Achieva Nova, Philips® MRI system, adjusting the antennas to the anatomic area and to the size of the tumor under study. In most patients, the conventional MRI protocol consisted of a set of a T1-weighted spin-echo sequence, a T2-weighted turbo spin-echo sequence and Proton Density-Spectral Attenuated Inversion Recovery (PD-SPAIR) imaging in the axial plane, and a T1-weighted spin-echo sequence in the long axis of the tumor (coronal or sagittal plane). Subsequently, 0.1 mmol/kg gadolinium was intravenously administered to the patient, and a T1-weighted spin-echo sequence was acquired in the axial axis and in the long axis of the tumor (MRI with static contrast). Diffusion-weighted MRI and perfusion MRI were additional sequences acquired in some patients. Diffusion-

weighted MRI was acquired in the axial plane, using a planar single-shot-echo sequence and four factors b ($b = 0, 300, 600, \text{ and } 1000 \text{ s/mm}^2$), followed by ADC mapping. For perfusion MRI, a T1 gradient echo sequence was acquired in the axial plane, with a first baseline set without contrast. During the 4 min after injecting the contrast, sets were recorded with acquisition times ranging from 6 to 10 s. The administered dose was 0.2 mmol/kg of body weight with an injection pump and a flow rate of at least 3 mL/second. In perfusion MRI studies, images were subsequently acquired with static contrast.

Evaluation of the MR images

MR images were independently evaluated by two radiologists, both of whom with more than 15 years of experience in musculoskeletal radiology. The cases were anonymized and randomly presented without access to clinical or histological data. The following tumor variables were analyzed in conventional MRI: depth, size (long axis), margins, signal intensity relative to muscle on T1, T2, and DP-SPAIR, signal homogeneity on these sequences, and presence of peritumoral edema and fat rim and/or cap. Superficial lesions are located in the skin and subcutaneous cellular tissue; deep lesions are differentiated into intramuscular and intermuscular lesions. The peritumoral edema corresponds to a hyperintensity on T2 in the periphery of the tumor. The fat rim and cap are a hyperintensity on T1, bordering the entire lesion or the apical and caudal poles, respectively.^{16,17}

The following MRI variables with static contrast were analyzed: enhancement pattern of tumor and enhancement of peritumoral edema.

The following DW-MRI variables were analyzed: homogeneity of diffusion restriction and global and solid ADC values. Apparent diffusion coefficient values were calculated using the Philips® workstation and two positioning systems of the region of interest (ROI), as shown in Figure 1, defining the global and solid ADC. The first positioning system was defined from a manually draw ROI covering the entire lesion in central sections (global ROI) and the second according to Nagata,⁹ using two ROI drawn in solid areas inside the tumor (solid ROI), which correspond to hyperintense regions in the b1000 sequence. The mean ADC value of each ROI was calculated, and in the solid ADC value, we calculated the mean value averaging the two mean values of the solid ROI.

The following perfusion MRI parameters were used: type of time-intensity curve (TIC) according to the classification by Daniel¹⁸ and start of dynamic enhancement scan delay time between start of arterial and tumor enhancement (T_0), calculated using the Philips® T1 Perfusion software; manually drawing an ROI in an arterial vessel and one or more ROI in different areas of the tumor (Figure 2).

Statistical analysis

A database was created in Microsoft® Excel®. Each patient was assigned a random number. The qualitative variables were described using absolute frequencies, and quantitative variables using measures of central tendency and dispersion and

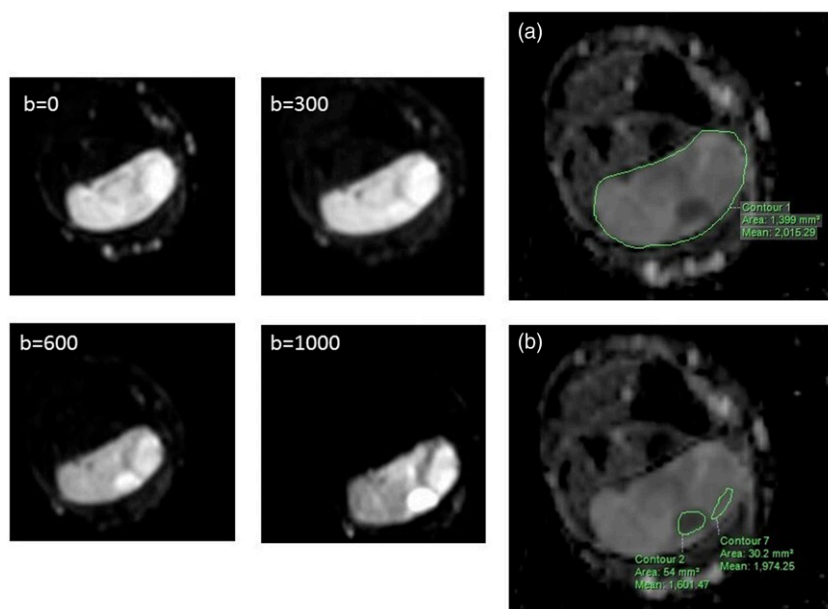


Figure 1. Diffusion sequences with four b -factors in a single axial plane to the left and ADC map to the right. ADC map with the calculation method of the numerical value of global ADC (A) and solid ADC (B). The solid ADC is obtained from the average value of two locations in the tumor with diffusion restriction in the b -factor = 1000.

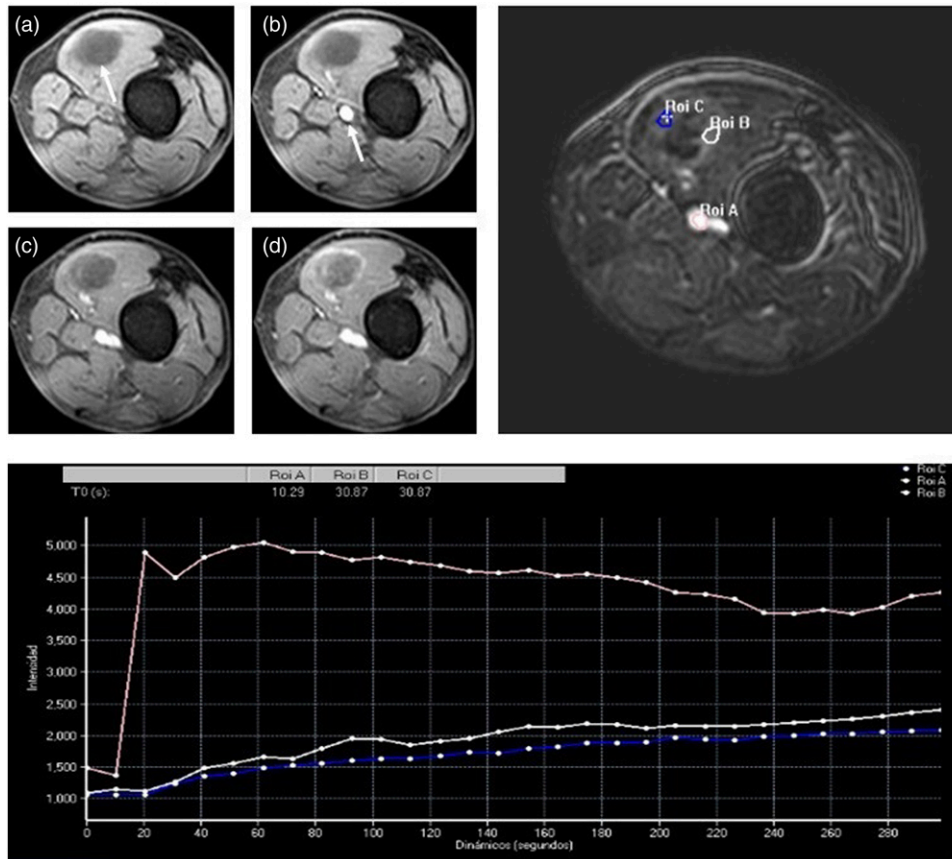


Figure 2. Perfusion MR exploration in a myxoma in vastus lateralis muscle. Up to the left (a–d), the same axial plane is shown four times: (a) prior to intravenous injection of contrast, show the tumor (arrow); (b) 30 s after arrival of bolus of gadopentetate dimeglumine, the enhancement of the femoral artery is appreciated (arrow); (c) at 2 min, and (d) 4.5 min that show the diffuse enhancement of tumor. Up to the right, with all dynamic series acquired, we draw one ROI in the femoral artery (ROI A) and two ROIs in the tumor (ROIs B and C). At the bottom, the time-intensity curve (TIC) is shown. The enhancement curve of the femoral artery is represented in pink, and the ROI in tumor is represented in white and blue. The curves are type II and with T0 or delay time of 20”.

analyzing the Receiver Operating Characteristic (ROC) curve of each calculation system of the ADC. If the area under the curve was greater than 70%, the optimal cut-off point was estimated using the Liu method assessing its validity for the diagnosis of MLPS. The area under the curve was expressed with its 95% confidence interval. The interobserver agreement was analyzed using the kappa index of the variables of conventional and contrast-enhanced MRI. Values lower than 0.4 were considered low; 0.4–0.59, moderate; 0.6–0.74, good; and 0.75–1, very good agreement. Statistical analysis was performed using the Stata program version 15.

Results

Patients

Of 21 patients with a histological diagnosis of myxoma or MLPS in extremities, four were excluded from the study: two with myxoma and another two with MLPS because the

MRI studies had been performed after the surgery. The final study sample included 17 patients, 10 with myxomas and 7 with MLPS. The patients with myxomas were six women and four men, with ages ranging from 34 to 72 years and with a mean age and standard deviation of 56 ± 14 years, and the patients with MLPS were four women and three men, aged from 30 to 78 years, with a mean age and standard deviation of 47 ± 16 years. The patients presented with a painless palpable mass, except in two patients with myxomas and 1 with MLPS, who visited the hospital for pain. Slow-growing lesions (more than 6 months of progression) were identified in all cases except for two myxomas and two MLPS. All tumors were in the lower limbs, except for two myxomas in the upper limbs.

Conventional MRI analysis

These results are outlined in Table 1. Both myxomas and MLPS were deep and had well-defined margins. No

Table 1. Results of MRI parameters for the radiologist I and interobserver agreement (κ).

Parameter	Myxoma (n = 10)	MLPS (n = 7)	κ
Location			
Intramuscular	8	4	
Intermuscular	2	3	
Longest diameter (cm)			
<5 cm	6	1	
5–10 cm	4	1	
>10 cm	—	5	
Margins			
Well defined	10	7	1
Ill defined	—	—	
T1 signal intensity*			
Hypointense	9	—	1
Isointense	1	1	
Hyperintense	—	6	
T2 signal intensity*			
Hypointense	—	—	1
Isointense	—	—	
Hyperintense	10	7	
DP-SPAIR signal i.*			
Hypointense	—	—	1
Isointense	—	—	
Hyperintense	10	7	
T1 homogeneity			
100% homogeneous	10	—	0.96
<50% inhomogeneous	—	4	
>50% inhomogeneous	—	3	
T2 homogeneity			
100% homogeneous	6	—	0.94
<50% inhomogeneous	4	5	
>50% inhomogeneous	-	2	
DP-SPAIR homogeneity			
100% homogeneous	7	—	0.93
<50% inhomogeneous	3	6	
>50% inhomogeneous	—	1	
Peritumoral edema			
Absent	2	5	0.41
Present	8	2	
Fat ring and/or cap			
Absent	2	4	0.74
Present	8	3	

*Signal intensity relative that of muscle.

myxoma was longer than 10 cm in long axis, whereas five of the seven MLPS were longer than 10 cm. The myxomas were predominantly intramuscular, and the MLPS were equally divided into intra- and intermuscular sarcomas. The peritumoral edema and the fat rim and/or cap were more commonly found in myxomas than in MLPS but were not exclusive to myxomas. In the T1 sequence, the myxomas were homogeneous and hypointense in relation to the muscle, whereas MLPS were predominantly heterogeneous

and had an intermediate signal intensity between that of muscle and fat. In T2 and DP-SPAIR sequences, both myxomas and MLPS were homogeneously hyperintense.

Static contrast-enhanced MRI analysis

The results are outlined in Table 2. Enhancement was predominantly nodular in MLPS and faint and diffuse in myxomas. Peritumoral edema was enhanced only in myxomas.

Table 2. Results of MRI characteristics with static contrast, diffusion and perfusion MRI for the radiologist 1, and interobserver agreement (κ).

	Myxoma	MLPS	κ
Static contrast MRI	(n = 9)	(n = 7)	
Pattern of enhancement			
Absent	1		0.62
Peripheral	2	—	
Diffuse	6	—	
Nodular	—	7	
Enhancement of peritumoral edema*	(n = 7)	(n = 2)	0.74
Present	6	—	
Absent	1	2	
Diffusion MR and ADC map	(n = 7)	(n = 3)	
Restriction			0.58
Homogeneous	6	—	
Heterogeneous	1	3	
Solid ADC ($\times 10^{-3}$ mm ² /s)	2.45 \pm 0.18	1.97 \pm 0.15	
Global ADC ($\times 10^{-3}$ mm ² /s)	2.38 \pm 0.15	2.14 \pm 0.25	
Perfusion MR	(n = 6)	(n = 2)	
Start of enhancement (t_0)			
≤ 8 s	—	2	
> 8 s	5	—	
None	1	—	
Progression of enhancement: TIC type			
I (none)	1	—	
II (gradual increase)	5	—	
III (Rapid with plateau)	—	1	
IV (Rapid with washout)	—	—	
V (rapid and sustained enhance)	—	1	

ADC values are the mean and \pm standard deviation.

*Only cases that had presented peritumoral edema on conventional MRI were taken into account.

Diffusion-weighted MRI analysis and ADC mapping

The results are outlined in Table 2, for seven myxomas and three MLPS. Heterogeneous diffusion restriction was identified in MLPS and only in one myxoma. Solid and global ADC values were higher in myxomas.

Table 3 presents the results of ROC curves. The area under the curve was greater than 70% for both ADC values; however, only the solid ADC cut-off point was selected. Figure 3 shows the solid ADC value of each tumor in relation to the cut-off point, 2.06×10^{-3} mm² x s, highlighting that the solid ADC values correctly classified myxomas and MLPS.

Perfusion MRI analysis

The results are outlined in Table 2, with type I (no enhancement) and type II (gradual increase) time-intensity (TIC) curves in myxomas and type III (rapid early enhancement followed by a plateau phase) and type V (rapid and sustained enhancement) curves in MLPS, whereas T_0 was longer than 8 s in myxomas and shorter in MLPS.

Interobserver agreement

The degree of interobserver agreement was 100% in margin definition, in T1, T2, and DP-SPAIR signals. The degree of interobserver agreement was very good in the assessment of T1, T2, and DP-SPAIR homogeneity and moderate in the assessment of the fat rim/cap. However, the agreement was low in the assessment of peritumoral edema, enhancement pattern, and diffusion restriction homogeneity/heterogeneity (Tables 1 and 2).

Discussion

Myxomas and MLPS share abundant myxoid material. For this reason, differentiating these tumors poses a challenge to radiologists. In addition, their prognosis differs considerably, that is, myxomas are cured with marginal resection, whereas MLPS require a combined treatment based on surgical excision with disease-free margins and chemoradiotherapy. Nevertheless, MLPS have a high risk of local and distant recurrence, with a mortality of approximately 25–40%.⁴

In our series, the demographic variables, age and sex of the patient, and the clinical presentation did not differ between the two tumors. Both are more frequent in women and have an average age at onset between the fifth and sixth decade of life. Clinically, they manifest as painless, slow-growing masses in the lower limbs, especially in the thighs. Difference in tumor size at presentation has been detected between myxomas and MLPS. Myxoid liposarcomas are larger than myxomas, exceeding 10 cm.

The conventional MRI criterion in our study that best differentiated myxomas from MLPS was the T1 signal

intensity. Myxomas show a homogenous and markedly hypointense signal in relation to the muscle (Figure 4), whereas MLPS show a heterogeneous signal. This difference can be explained because myxomas only show myxoid content with a signal intensity equal to that of the liquid. Nevertheless, in T2 and DP-SPAIR (sequences with long relaxation times), no significant differences were found between these tumors, which are highly hyperintense and show a pseudocystic appearance, which hides the small, less hyperintense or hypointense fat foci or septa that MLPS may present.

Other MRI features such as the fat rim and peritumoral edema that are considered quite specific of myxomas,¹⁹ they were presented in both tumors in our series. Nonetheless, the fat rim was most prominently at the superior and inferior poles of the myxomas, whereas the fat rim was around all the lesions in the MLPS. In the myxomas, the fat represents the atrophy of the adjacent muscle, and in the MLPS, the rim of fat is secondary to displacement of the intermuscular fatty connective tissue by the tumor, known to split fat sign. This sign is not specific to MLPS and can be seen with any mass arising in an intermuscular location.²⁰

Regarding, the peritumoral edema has been the rule in the myxomas and less frequent in MLPS in our series. In

Table 3. Results of ROC curves in analysis of ADC values.

	Global ADC	Solid ADC
Area under ROC (CI 95%)	0.83 (0.51–1)	1 (1)
Optimal cut-off point ($\times 10^{-3}$ mm ² /s)		2.06
Sensitivity*		1
Specificity*		1

CI: confidence interval.

*Optimal cut-off point for the diagnosis of MLPS.

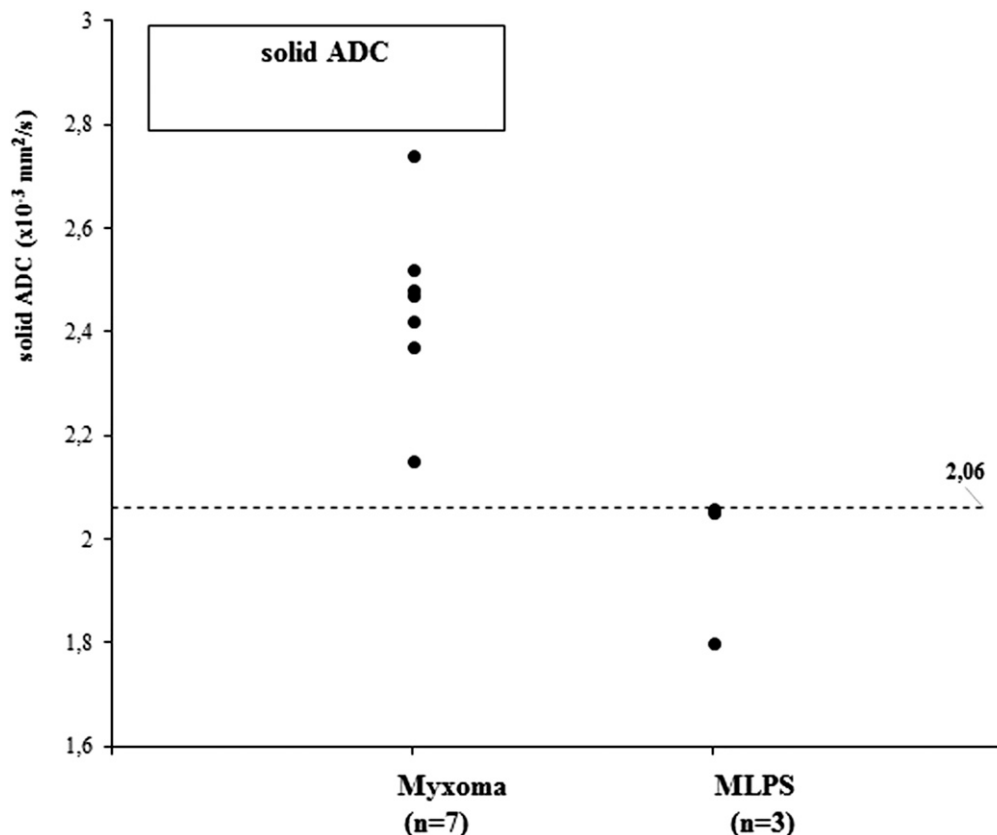


Figure 3. Dot plot of solid ADC values. Each dot corresponds to the ADC values obtained in our case series. The dashed line represents the threshold value obtained in the ROC analysis for solid ADC measurement system.

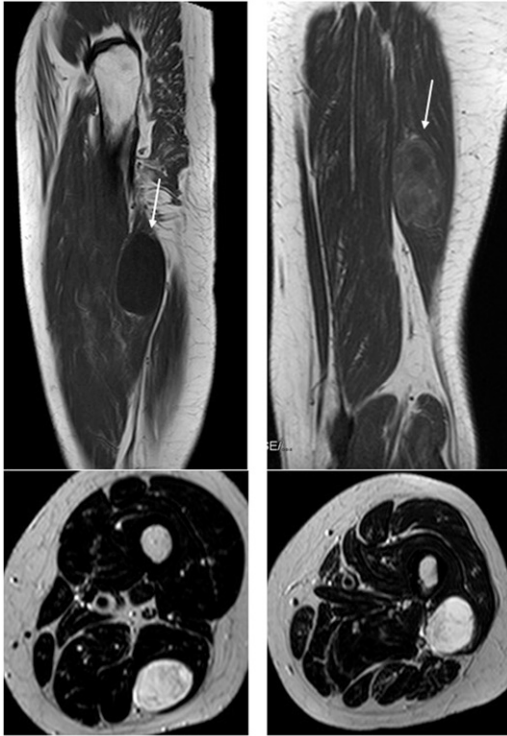


Figure 4. Coronal T1 weighted (images at the top) and axial T2 weighted (images at the bottom). In the left, the lesion is homogeneously hypointense on T1 and heterogeneously hyperintense on T2 (myxoma); in the right, the lesion is heterogeneously on T1 and T2, (MLPS).

the myxomas, the edema corresponds to the myxoid content drained to the contiguous soft tissue,²⁰ while in MLPS as other sarcomas, the peritumoral edema is compressive or infiltrative. Furthermore, there were peritumoral edema enhancement at T1 after gadolinium injection in myxomas and there was not contrast enhancement beyond the tumor borders in MLPS. In the literature, the presence of peritumoral contrast enhancement is a feature that may be solely used to diagnose high histological grade of STTs.^{21–23} In our series, five MLPS were grade 1 or low and two grade 2 or intermediate according to the French Federation of Cancer Centers histologic grading system. In these low or intermediate histological grade sarcomas, the edema peritumoral is neither compressive nor tumoral infiltration.

However, the peritumoral enhancement of the myxomas was diffuse and quite homogeneous like that of the myxoma itself.

Gadolinium behavior was very typical of both tumors with faint, diffuse, and homogeneous enhancement for myxomas (Figure 5) and with a heterogeneous, nodular, and predominantly peripheral enhancement in MLPS.^{5,24–26} In perfusion, the myxomas enhanced gradually over the first minutes with centripetal filling (swirling internal

appearance), whereas the MLPS showed prominent and rapid enhancement.

Our DW-MRI findings are preliminary, given our small sample size, but promising. Among the studies reviewed for this research, the myxoid tumor results differ, most likely because their authors use different methods for calculating ADC values. More specifically, those methods differ in the ROI used to calculate ADC values; Einarsdottir uses an ROI of the entire section of the tumor in its largest diameter, Maeda uses an ROI circumscribed to a focus with a solid aspect inside the tumor, and others such as Nagata use ROIs in two solid foci and calculate the mean of the resulting ADC values.^{6,8,27} These three authors use the mean ADC value of the ROI, unlike others who selected the minimum ADC value (representing the highest degree of cellularity).^{11,12}

In the present study, we compared two methods for calculating ADC values as a function of the ROI, solid and global ADC (Figure 1). In MLPS, solid ADC values were lower than global ADC values because the ROI of a solid ADC corresponds to hypercellular foci, whereas the global ROI contains myxoid tissue. Global ADC does not allow to establish a cut-off point for diagnosis MLPS, whereas the solid ADC assessing cut-off point with 100% sensitivity and specificity

Figure 6 shows the ADC results of our and other series reported in the literature in comparison with our cut-off point ($2.06 \times 10^{-3} \text{mm}^2 \text{xs}$). Myxomas and other benign myxoid tumors and MLPS and other malignant myxoid tumors are correctly classified when using solid ADC values in our series and in the others. The clinical misdiagnosis of malignant tumors as benign, in our case confusing MLPS with myxomas, is the error that we intend to avoid because this has the worst consequences for the patient. Therefore, global ADC does not allow to establish a cut-off point for diagnosis of MLPS.

Our study has several limitations. The main limitation is its small sample, which results from the low incidence of the tumors under investigation. This low incidence limits the reproducibility and external validity of our results. Hypothesis contrast tests were not performed, and thus all differences found may not necessarily be significant. This was a retrospective study and, as such, lacked standardized (clinical or pathological) data collection or MR imaging protocols. Diffusion-weighted and perfusion studies were only performed in some patients. The interobserver agreement in conventional MRI parameters was, in general, good or very good, but the peritumoral edema, a sign evaluated in T2, showed the lowest degree of agreement. In this research, the T2 sequences were acquired in the axial plane, which could have made their detection difficult. In future studies, T2 sequences should be acquired in the long axis of the tumor (coronal or sagittal plane). The DW-MRI analysis of our study was restricted to a specific clinical

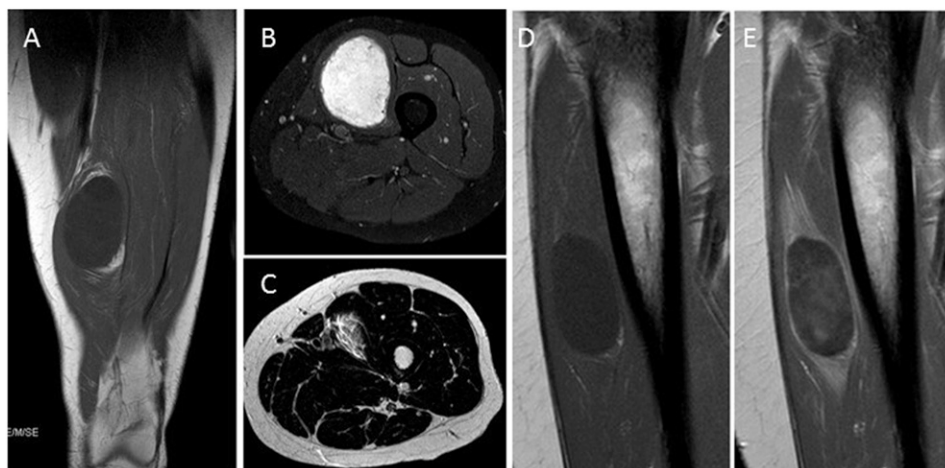


Figure 5. Intramuscular myxoma. T1-weighted sequence (A) reveals ovoid, well-defined, homogeneously hypointense lesion with fat cap. DP-SPAIR (B) and T2-weighted sequence (C) show hyperintense lesion with peritumoral edema. T1-weighted, before (D) and after (E) injection of contrast material presents the diffuse enhancement of the tumor and the peritumoral edema.

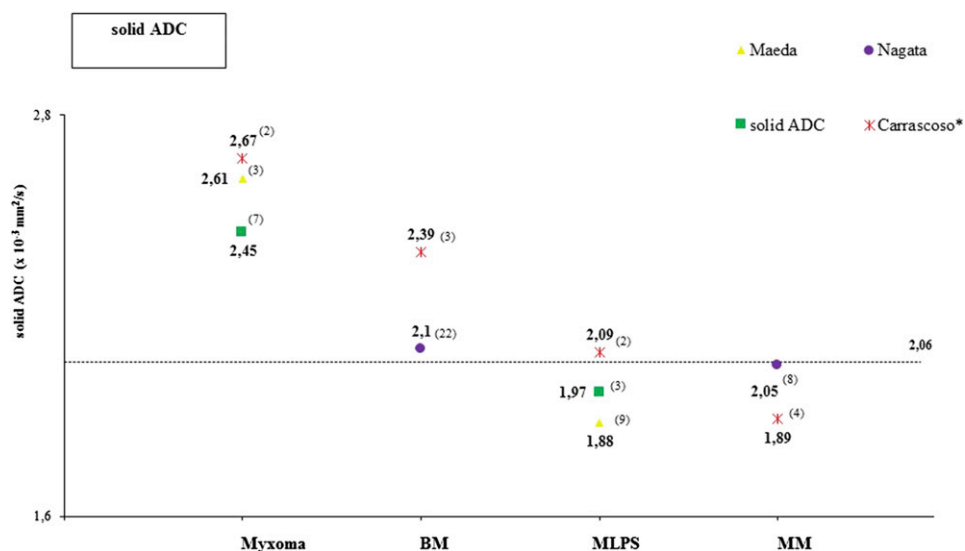


Figure 6. Dot plots of solid ADC in different cases series. Each dot represents the mean and median ADC values of each series (legend) for myxomas, benign myxoid tumors (BM), MLPS, and malignant myxoid tumors (MM). Our results are represented by the squares. The number of cases of each series is right to each dot in parentheses. The dashed line represents the threshold value obtained in our study.

situation, requiring us to differentiate only between two types of tumors and, therefore, facilitating the identification of differences. The results from ROC curve analysis may be due to the small sample size. All studies published thus far, including ours, used a monoexponential diffusion model that does not differentiate real diffusion (without the perfusion effect) even though we used up to four b values to reduce the contribution of perfusion to the ADC value. The plotted ROIs varied in size, and the possible size effect on the calculation of the ADC values has not been analyzed.

Although more complex analyses of diffusion-weighted and perfusion techniques are available, the parameters chosen in this study are quickly acquired and easily interpreted and therefore can be easily incorporated into daily practice. The results must be interpreted with caution, especially in clinical work, where the range of diagnostic possibilities is broader: to differentiate myxomas from MLPS. We propose to conduct a multicenter and prospective study, with a larger sample size, including other types of myxoid tumors, a standardized imaging protocol, and the involvement of

pathologists to correlate the MRI with histological findings. For example, the ADC value could be useful in differentiating MLPS with a higher histological grade or the cellular variant of intramuscular myxomas.

In conclusion, treating patients with a deep, lower-limb myxoid-like tumor requires excluding MLPS. In the absence of any other clinical or imaging features of malignancy, an intramuscular myxoma is a likely option. Despite having a similar clinical presentation and sharing a pseudocystic radiological appearance, myxomas and MLPS differ in all MRI modalities, as found in our study. The following parameters best differentiated both tumors: a size greater than 10 cm in MLPS, homogeneous T1 hypointensity in myxomas, enhancement of peritumoral edema in myxomas, and nodular enhancement in MLPS. However, other criteria such as margins, T2 signal (or long TR sequences), peritumoral edema, and fat rim/cap were not discriminative. The analysis of ADC values in diffusion, as well as TIC curves in perfusion, is relatively simple and fast procedures that assist the radiologist. Incorporating ADC values, especially solid ADC values, may improve sensitivity in MLPS diagnosis, albeit at the expense of increasing the number of false positives. The latter could be avoided by considering other MR modalities. Therefore, each modality has its limitations, and combining all modalities should increase diagnostic precision.

Declaration of conflicting interests

The author(s) declared no potential conflicts of interest with respect to the research, authorship, and/or publication of this article.

Funding

The author(s) received no financial support for the research, authorship, and/or publication of this article.

ORCID iDs

Luz M Moran  <https://orcid.org/0000-0001-7740-0836>

Jesus Vega  <https://orcid.org/0000-0001-6844-9697>

References

1. Willems SM, Schrage YM, Baelde JJ, et al. Myxoid tumours of soft tissue: the so-called myxoid extracellular matrix is heterogeneous in composition. *Histopathology* 2008; 52: 465–474.
2. Heymans O, Gebhart M, Alexiou J, et al. Intramuscular myxoma. *Acta Chir Belg* 1998; 98: 120–122.
3. Muratori F, Bettini L, Frenos F, et al. Myxoid liposarcoma: prognostic factors and metastatic pattern in a series of 148 patients treated at a single institution. *Int J Sur Oncol* 2018; 6: 1–9.
4. Jo VY and Hornick JL. Tumors with myxoid stroma. In: Hornick JL (ed). *Practical soft tissue pathology: a diagnostic approach*. 2nd ed.. Philadelphia, PA: Elsevier, 2018, pp. 135–163.
5. Petscavage-Thomas JM, Walker EA, Logie CI, et al. Soft-tissue myxomatous lesions: review of salient imaging features with pathologic comparison. *Radiographics* 2014; 34: 964–980.
6. Einarsdóttir H, Karlsson M, Wejde J, et al. Diffusion-weighted MRI of soft tissue tumours. *Eur Radiol* 2004; 14: 959–963.
7. Jeon J Y, Chung HW, Lee MH, et al. Usefulness of diffusion-weighted MR imaging for differentiating between benign and malignant superficial soft tissue tumours and tumour-like lesions. *Br J Radiol* 2016; 89: 20150929.
8. Maeda M, Matsumine A, Kato H, et al. Soft-tissue tumors evaluated by line-scan diffusion-weighted imaging: influence of myxoid matrix on the apparent diffusion coefficient. *J Magn Reson Imaging* 2007; 25: 1199–1204.
9. Nagata S, Nishimura H, Uchida M, et al. Diffusion-weighted imaging of soft tissue tumors: usefulness of the apparent diffusion coefficient for differential diagnosis. *Radiat Med* 2008; 26: 287–295.
10. Vilanova J C, Luna A, Baleato S, et al. Aplicaciones de la técnica de difusión por resonancia magnética en el manejo de la patología tumoral osteomuscular. *Radiologia* 2012; 54: 14–26.
11. Chabra A, Ashikyan O, Slepicka C, et al. Conventional MR and diffusion-weighted imaging of musculoskeletal soft tissue malignancy: correlation with histologic grading. *Eur Radiol* 2019; 29: 4485–4494.
12. Lee JH, Yoon YC, Seo SW, et al. Soft tissue sarcoma: DWI and DCE-MRI parameters correlate with Ki-67 labeling index. *Eur Radiol* 2020; 30: 914–924.
13. Carrascoso J, Acevedo A, Herraiz L, et al. Utility of diffusion in bone and soft tissue tumors. ADC-Histological findings correlation. In: XXXII National Congress of the Spanish Society of Medical Radiology–SERAM, Oviedo, Spain, 2014.
14. Choi Y J, Lee I S, Song Y S, et al. Diagnostic performance of diffusion-weighted (DWI) and dynamic contrast-enhanced (DCE) MRI for the differentiation of benign from malignant soft-tissue tumors. *J Magn Reson Imaging* 2019; 50: 798–809.
15. Moustafa A, Eldaly M M, Zeitoun R, et al. Is MRI diffusion-weighted imaging a reliable tool for the diagnosis and post-therapeutic follow-up of extremity soft tissue neoplasms? *Indian J Radiol Imag* 2019; 29: 378–385.
16. Baheti AD, Tirumani SH, Rosenthal MH, et al. Myxoid soft-tissue neoplasms: comprehensive update of the taxonomy and MRI features. *Am J Roentgenol* 2015; 204: 374–385.
17. Bancroft LW, Kransdorf MJ, Menke DM, et al. Intramuscular myxoma: characteristic MR imaging features. *Am J Roentgenol* 2002; 178: 1255–1259.

18. Daniel BL, Yen YF, Glover GH, et al. Breast disease: dynamic spiral MR imaging. *Radiol* 1998; 209: 499–509.
19. Luna A, Martinez S and Bossen E. Magnetic resonance imaging of intramuscular myxoma with histological comparison and a review of the literature. *Skeletal Radiol* 2005; 34: 19–28.
20. Murphey MD, McRae GA, Fanburg-Smith JC, et al. Imaging of soft-tissue myxoma with emphasis on CT and MR and comparison of radiologic and pathologic findings. *Radiol* 2002; 225: 215–224.
21. White LM, Wunder JS, Bell RS, et al. Histologic assessment of peritumoral edema in soft tissue sarcoma. *Int J Radiat Oncol Biol Phys* 2005; 61(5): 1439–1445.
22. Zhao F, Ahlawat S, Farahani S, et al. Can MR imaging be used to predict tumor grade in soft-tissue sarcoma? *Radiol* 2014; 272(1): 192–201.
23. Crombe A, Marcellin P-J, Buy X, et al. Soft-tissue sarcomas: assessment of MRI features correlating with Histologic Grade and patient outcome. *Radiol* 2019; 291: 710–721.
24. Sung MS, Kang HS, Suh JS, et al. Myxoid liposarcoma: appearance at MR imaging with histologic correlation. *Radiographics* 2000; 20: 1007–1019.
25. Manaster BJ. Soft-tissue masses: optimal imaging protocol and reporting. *Am J Roentgenol* 2013; 2: 505–514.
26. Crombe A, Alberti N, Stoeckle E, et al. Soft tissue masses with myxoid stroma: can conventional magnetic resonance imaging differentiate benign from malignant tumors? *Eur J Radiol* 2016; 85: 1875–1882.
27. Van Rijswijk CS, Geirnaerd MJ, Hogendoorn PC, et al. Soft-tissue tumors: value of static and dynamic gadopentetate dimeglumine-enhanced MR imaging in prediction of malignancy. *Radiol* 2004; 233: 493–502.